SIXTH FRAMEWORK PROGRAMME
Nanotechnologies and nano-sciences, knowledge-based multifunctional materials and new production processes and devices –NMP

FP6-2003-NMP-NI-3

Proposal n° 515810-2

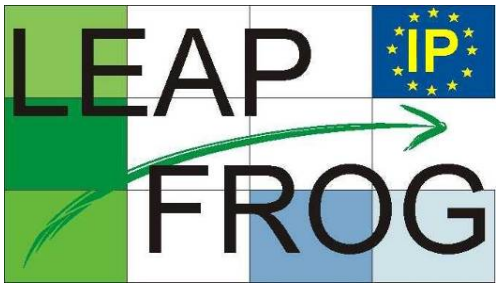

Leadership for European Apparel Production From Research along Original Guidelines

D4.19 Results of feasibility study for classification of fabrics and quick automatic estimation of their simulation parameters based on Image Analysis

Identifier

Date:	31.01.08
Author(s):	Harris Georgiou, G.A. Kartsounis (members of the team of AUA, subcontractor to Hohenstein Institute), Corresponding author: Harris Georgiou, University of Athens (Email: xgeorgio@di.uoa.gr
Distribution[1]:	
Workpackage:	WP4
Status	Final
Abstract	This report summarises the methodology and the findings of the feasibility study conducted in the framework of Task 4.1 – "Material characterization for simulation and fabric selection" - Sub-task 4.1.4: Image Analysis Techniques for Material Characterization and Simulation"

[1] All partners, WP1 participants

Table of Contents

1. Introduction

1.1 Purpose

This report describes an extensive summary of the results Sub-task 4.1.4: Image Analysis Techniques for Material Characterization and Simulation", a research activity of Task 4.1 – "Material characterization for simulation and fabric selection" related to the fast and efficient estimation of fabric simulation parameters, currently being identified by long, expensive and not entirely objective measuring techniques (Kawabata, FAST, ..). The task aimed at the automatic comparison of the shape of fabric drape of a sample of an unknown fabric with that of the drape of known fabrics in the Fabrics Library (see D4.1, D4.2: Simplified Method to identify Material Characteristics) based on image analysis of their corresponding projections when lying on a standard circular base (extension of the Cusic drapemeter). The original idea was the combination of the simple drape meter apparatus with sophisticated Image Analysis and state-of-the-art ***statistical learning algorithms*** could lead to the development of an innovative technique for the fast evaluation of the simulation parameters for any unknown fabric leading to faster and easier adoption of Virtual Prototyping by the industry.

The work description in Annex 1 (M12-M30) included:

- The identification of image features for a reliable representation of the projections of fabrics draped on the standard circular substrate.
- The definition of Methodology for Image Analysis.
- First experiments with existing sample images of single layer fabrics
- A feasibility study to estimate the efficiency of similarity metrics based on an efficient model representation of the drape image boundary in order to classify fabrics based on their draped projections and their subsequent comparison to standard drape images stored in the Fabrics Library.

1.2 Objectives and scope

Previous work by Hohenstein involved the definition and development of a novel simplified, fast and efficient technique for the characterisation of fabrics in terms of their mechanical properties affecting the drape of the garment (the way the garment falls over the body). In co-operation with other partners they have developed a Fabrics Library

including key mechanical parameters of a number of reference fabrics accompanied by representative images of the shadows of fabric samples draped over a circular support (simplified version of the Cusic drapeometer, see picture). The required mechanical parameters (such as weight, thickness, shearing rigidity, bending rigidity elasticity and formability) which are currently used for the analysis, are measured by standard laboratory equipment (e.g. Fast, Kawabata, etc) in a process that is tedious and costly. The general idea of the simplified method currently being developed by the Institute is to attempt to derive for each new fabric the parameters required for the realistic simulation of a garment to be constructed with the new fabric

during the virtual prototyping phase by a simple, fast, completely automatic and robust technique.

Features, such as the number of folds, characteristics of folds, size of the area etc, are currently used for the visual comparison of a typical drape shadow of the unknown fabric (see picture on the side) to relevant images of reference fabrics with known physical parameters stored in the Fabrics library.

One of the important findings of the original work by Hohenstein was that the determination of concrete correlations between fall and draping of garments and their tracing back to physical parameters by using simple features, such as the number of folds as well as subjective visual classification of the drape image shapes was more complex than expected. The results showed that the draping behaviour of single and multi-layered material of fabrics ***could not be modelled reliably by considering a few isolated features of the drape boundary.*** These simple features showed non-repeatability, i.e. they varied between different instances of the draping of the same fabric under different conditions in a random manner. The first results of this manual observation resulted in an ad hoc subjective classification of the obtained drape boundaries in a number of classes which proved non representative of the sample of known fabrics.

A need therefore arose to model the drape boundary by a more information rich statistical representation which could only be obtained by a statistically based objective evaluation of a large number of instance invariant features obtained by automatic image analysis and statistical inference.

1.3 Background

Shape analysis is one of the most common problems encountered in the disciplines of Pattern Recognition and Machine Learning in general. Shape representation is focused on the problem of identifying and encoding important properties of an object's boundary information or boundary plus interior content. A wide range of shape descriptors have been designed for a variety of applications, including shape signatures, signature histograms, shape invariants, boundary moments, zero-cross count, curvature, spectral shape features, etc [R01,R05,R06].

Shape representation methods can be organized into two main categories [R01], namely: (a) *contour-based* techniques and (b) *region-based* techniques. Contour-based techniques exploit *structural* information of the object's boundary by analyzing the corresponding 1-D signal and encoding it with chain codes, invariants, etc, or analyzing global statistics of the signal by means of perimeter (in case of convex shapes), zero-crossing counts, entropy, 1-D fractal analysis, Fourier descriptors (spectral representation), Wavelet analysis (multi-scaled representation), roughness index, B-splines, snakes (interpolation), etc. Region-based techniques exploit the properties of the object's content, including global statistics such as area, area ratio parameter (in case of convex shapes), eccentricity, etc, or structural information such as convexity, principal axes, etc. Table 1 illustrates the categorization of some of the most commonly used contour- and region-based shape descriptors.

Recent studies [R11] have already shown that spectral representation and wave analysis of the boundary signal is a very efficient way to compare and categorize the shape of the drape shadow into one of the known classes in the Fabrics library. However, the aspect of spectral or wave analysis of the 1-D drape signal has been studied only in the context of Fourier analysis and only in the form of area ratios between the original and the FFT representations of the signal. Furthermore, the dominant property of the drape shape boundary signal exploited in the current practices is the number of distribution of the wave "peaks" [R11].

Table-1: Categorization of some of the most commonly used contour-based and region-based shape descriptors.

Shape Descriptors			
Contour-based		**Region-based**	
Structural	**Global**	**Global**	**Structural**
Chain code Invariants Polygon B-splines Snakes ...	Perimeter Zero-crossings Entropy Fractal analysis Fourier descriptors Wavelet analysis Roughness index ...	Area Area Ratio Eccentricity Zernike moments Legendre moments ...	Convexity Principal axes ...

Optional Methodologies

It is clear that numerous of these generic shape descriptors can be employed to encode the various aspects and dominant properties of the 1-D boundary signal of the convex shape in a robust and very effective way. In particular, shape descriptors such as signal roughness index, fractal analysis, zero-crossing count, entropy, etc, can provide very useful and detailed information about the boundary signal itself.

Furthermore, thorough spectral representation and analysis of the boundary signal by means of Fourier power spectrum techniques and Fourier descriptors, as well as multi-resolution spectral representation via wavelet analysis (e.g. modulus-maxima representation [R04]), can reveal significant properties of the 1-D signal at various scales. Since the drape shape is a convex form, many more shape descriptors can be employed in the context of region-based techniques, including area ratio parameter, eccentricity, boundary moments, etc.

This is clearly a significant improvement of the simple area-ratio measurements currently used for the characterization of a drape shadow image [R11].

Similar techniques have been used very successfully in similar problems of shape analysis, combined with content-rich object (texture) recognition, such as the automated detection and classification of mammographic masses [R02,R03,R05,R10].

A large set of effective and robust shape descriptors can be selected in an optimal way, employing statistical significance tests (such as MANOVA [R12]) against a specific

classification target, e.g., a set of drape shape categories. These shape features can be used as the base training dataset for any decision-theoretic classification model.

Specifically, these datasets can be partitioned and used appropriately to train a linear classifier [R08], such as Least-Squares Minimum Distance (LS-MDC) or Linear Discriminant Analysis (LDA), in order to automatically predict the correct category for a new drape shape image of unknown classification. Furthermore, more complex classification tasks can be addressed by more robust and efficient non-linear classifiers [R08], such as k-nearest-neighbor (k-NN), Bayesian and Neural Networks (NN).

All these models have been used extensively in the last few decades in the discipline of Pattern Recognition to address classification problems of high complexity and dimensionality, in a very wide range of applications including object recognition [R13], computer-aided diagnosis (CAD) [R02,R03,R05,R10], optical character recognition (OCR) [R13], etc.

Recent advances in Statistical Learning and Decision Theory have established a well-founded mathematical framework for very efficient learning models, such as the Support Vector Machine (SVM) and kernel machines in general [R14]. SVM classifiers that employ various non-linear kernels, combined with new algorithms for fast training of these architectures, are considered state-of-the-art in Pattern Recognition today [R14,R09] and they can be regarded as a realistic upper limit in the performance of automated systems for similar applications in practice.

Multi-class categorization problems, such as the case of the Fabrics library, are often addressed by employing ensembles of simpler classifiers, typically one for each class, instead of one classifier for the complete N-class problem. Designing optimal combination schemes of multiple classifiers is a very active research area in Pattern Recognition today and there are many well-studied combination methods that have been used successfully in the past [R08]. Furthermore, there is a wide range of possible optimization/training schemes for these combination models, from simple rank-based and simple majority rules [R15], optimal weighted average and weighted majority rules [R07], cascaded ensembles of classifiers [R15], mixture of experts [R15], to the commonly used Boosting [R08] and Bagging [R08] methods. Since the drape shape categorization problem is indeed a well-formulated N-class classification problem, essentially all these methods can be employed for the implementation of a state-of-the-art system for automatic shape classification.

References:

[R01] D. Zhang, G. Lu, Review of shape representation and description techniques, Pat. Rec., 37 (2004) 1-19.

[R02] H. Li, Y. Wang, K.J.R. Liu, S.C.B. Lo, M.T. Freedman, Computerized radiographic mass detection – Part II: Decision support by featured database visualization and modular neural networks, IEEE Trans. Med. Im., 20 (4) (2001) 302-313.

[R03] J. Kilday, F. Palmieri, M.D. Fox, Classifying mammographic lesions using

computerized image analysis, IEEE Trans. Med. Im., 12 (4) (1993) 664-669.

[R04] L.M. Bruce, R.R. Adhami, Classifying mammographic mass shapes using the wavelet transform modulus-maxima method, IEEE Trans. Med. Im., 18 (12) (1999) 1170-1177.

[R05] H.D. Cheng, X.J. Shi, R. Min, L.M. Hu, X.P. Cai, H.N. Du, Approaches for automated detection and classification of masses in mammograms, Pat. Rec. 39 (2006) 646-668.

[R06] Q.M. Tieng, W.W. Boles, Recognition of 2D object contours using the wavelet transform zero-crossing representation, IEEE Trans. PAMI, 19 (8) (1997) 910-916.

[R07] H. Georgiou, M. Mavroforakis, S. Theodoridis , A Game-Theoretic Approach to Weighted Majority Voting for Combining SVM Classifiers, Int. Conf. on ANN (ICANN), 10-13 September 2006, Athens, Greece - Ref: S.Kollias et al. (Eds): ICANN 2006, Part I, LNCS 4131, pp. 284-292, 2006.

[R08] S. Theodoridis, K. Koutroumbas, Pattern Recognition, 3rd edition (Academic Press, San Diego, USA, 2006).

[R09] Mavroforakis, M., Theodoridis, S.: Support Vector Machine Classification through Geome-try. Proc. XII Eur. Sig. Proc. Conf. (EUSIPCO2005), Antalya, Turkey, Sep. 2005.

[R10] H. Georgiou, M. Mavroforakis, N. Dimitropoulos, D. Cavouras, S. Theodoridis, Multi-scaled morphological features for the characterization of mammographic masses using statistical classification schemes, Artificial Intelligence in Medicine, 2006 (in review for publication).

[R11] C.K. Park, S. Kim, W.R. Yu, Quantitative Fabric Drape Evaluation System Using Image Processing Technology (Part 1: Measurement System and Geometric Model), J. Testing and Eval., 32 (2) (2004)

[R12] W.W. Cooley, P.R. Lohnes, Multivariate data analysis (John Willey & Sons, New York, 1971).

[R13] R.C. Gonzalez, R.E. Woods, Digital Image Processing, 3rd edition (Prentice-Hall, New Jersey, 2006).

[R14] V.N. Vapnik, Statistical Learning Theory (John Wiley & Sons, New York, 1998).

[R15] L.I. Kuncheva, Combining Pattern Classifiers (John Wiley & Sons, New Jersey, 2004).

2. Materials and Methods

The task of drape image analysis, recognition and categorization consists of several subsequent procedures that are required to transform the initial color image to a set of well-defined invariant shape descriptors or "signature" for every drape category.

The overall process was organized into the following discrete phases:

- Model Assessment: Design of models and pre-processing stages for the drape images.
- Pre-Processing: Processing of the complete set of the drape images and acquisition of the selected shape descriptors.
- Categorization-Prediction: Design and implementation of predictive models regarding the correct recognition of some basic properties and/or physical parameters of the fabrics.

2.1 Phase-1: Model Assessment

The initial database consisted of 90 fabric drape samples, photographed at five realizations each, for a total of 450 sample fabric drape images. The samples were organized into three categories according to their layered characteristics, namely: ML for multi-layered, SL for single-layered and Q for others. Table 1 presents the distribution of fabric and image samples across this initial set.

Table 1: Distribution of fabric and image samples across the initial dataset.

Samples	Type: SL	Type: ML	Type: Q	TOTAL
fabrics	67	15	8	90
images	335	75	40	450

Since the purpose of this was to establish a basic methodology for automatic drape image analysis, only the simpler and larger subset was used, i.e., the SL. This image set was used as an image-related representation of the FL, along with the standard measurements, physical data and category memberships already contained in the FL [R99]. It should be noted that each drape image was considered as autonomous data sample, despite the fact that sets of five images were taken for each drape sample (same fabric). This assertion is valid since the shape descriptors should be invariant to different "realizations" of the same drape sample, i.e., should be able to closely match images (drape shapes) that correspond to the same drape sample (same fabric).

The first phase of this work was focused on the design and optimization of the "acquisition" procedures of drape shape properties, since these morphological characteristics are implicitly related to the physical properties of the fabric itself [R00, R11, R19]. Specifically, the assessment and evaluation of various models was organized into two major areas of interest:

1. Pre-processing filters for image restoration
2. Geometric correction for camera lens effects

The standard image pre-processing addresses typical image acquisition problems, including noise, motion blurring, non-uniformities of field (gain profile, flat-field correction), camera deficiencies (bad pixels), etc. These filters can be implemented as spatial convolution kernels or spectral filters, according to their desired response functions. In this study, the issues that were considered were only those related to noise and other spatial artifacts, since the geometry, equipment and experimental setup was fixed for the entire set of acquired images.

Geometric correction methods address the problems related to lens deficiencies and non-linearities, which are typically the results of using real cameras that do not correspond to the "perfect" pinhole camera model. In practice, the image is deformed geometrically through a set of well-defined transformations, including pincushion, barrel and perspective distortions. These transformations can be "inversed" by designing approximate of analytical models [R13]. In this study, the single most relevant issue identified was the barrel distortion, typical to all the commercial CCD-based digital cameras [R98]. Hence, an analytical model was employed for implementing a geometric correction filter, after the drape shape boundary was acquired.

Figure 1 presents the basic approach employed for the Model Assessment phase of this study. The labels *model.A1* and *model.A2* refer to the identified optimal designs for image pre-processing filters and geometric corrections, accordingly.

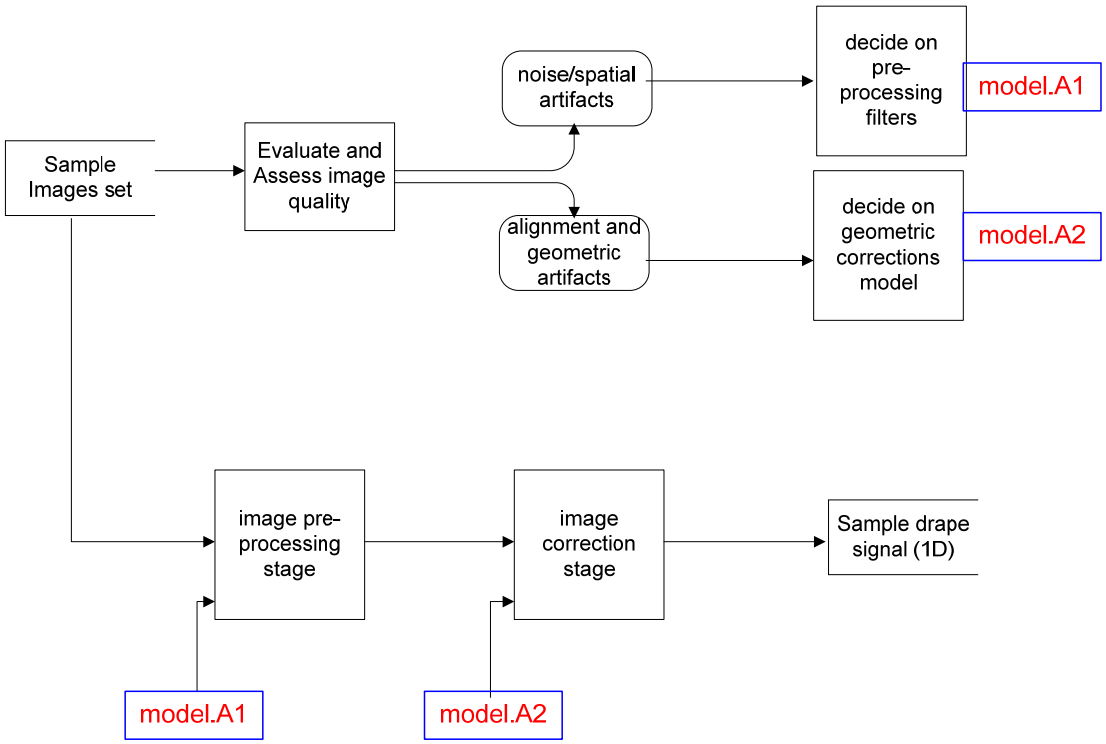

Figure 1: Basic approach employed for the Model Assessment phase of this study.

2.2 Phase-2: Pre-Processing

The Model Assessment phases of this work resulted in the design specifications of the optimized "pipeline" for processing the raw drape images and creation of a robust representation of the drape boundary shape, subject to further analysis in subsequent stages.

Using the *model.A1* and *model.A2* specifications of phase-1, these two protocols were implemented and applied on the entire drape image database. Specifically, a set of sub-processes were identified for each primary stage (pre-processing filters, geometric corrections) according to standard image processing techniques [R13].

For the pre-processing filters, the procedure included several "pipelined" spatial filters for region-based and morphological transformations, applied on each drape image separately. The exact sequencing and parameters of these sub-processes were identified and optimized after extensive experimentation:

1. Conversion of 24-bit RBG image to 8-bit grayscale
2. Resize/rescaling of the image
3. Cropping of image, extraction of Region-of-Interest (ROI)
4. Histogram normalization (contrast enhancement)
5. Identification of object center
6. Optimized histogram thresholding (segmentation)
7. Edge detection and tracing of drape boundary
8. Speckle removal (erosion filtering)
9. Non-continuities removal (dilation filtering)
10. Skeletonization (edge thinning)

The images were converted to grayscale (from RGB) in order to make them compatible with standard morphological transformations ("operators"). Rescaling ensured that all the images were processed at the same physical spatial resolution (corresponding to the 250 mm of the photographed plane). The downscale factor chosen was roughly x0.5 per dimension, resulting a spatial resolution of 5 pixels per mm (instead of 10 pixels per mm originally). Both these procedures contributed to a x10 to x12 speedup of the overall process, since the original drape image was reduced to 1/4 of its original size and 1/3 of its original bit depth, with no decrease of the significant morphological properties of the drape boundary itself.

The Region-of-Interest (ROI) was defined as the minimum rectangular box containing the complete drape object. This approach was necessary in order to isolate the most relevant portion of the drape image before any further processing, especially the contrast enhancement step that follows. The center of the drape object was identified both experimentally, using fixed measurements on the image and the equipment setup itself, as well as through an adaptive imaging technique, using the Radon transformations for multiple 1-D projections and the identification of mass center [R13]. Both approaches resulted in the correct identification of the center of the drape object with typical error of 1 mm or less, which was verified as acceptable for this particular study.

Using the properties of the grayscale histogram of the ROI, as well as the prior identification of the center of the drape object, an optimized histogram thresholding technique was employed to segment the drape object from its background with minimum loss of drape boundary pixels and noise artifacts. The thresholded drape object was subsequently converted to contour image using a standard edge detection filter (Sobel), which practically introduced the first rough "version" of the signal of interest, i.e., the drape boundary.

Several morphological operators were used for correcting and enhancing the contour signal before extracting any shape features. First, an erosion step was employed for speckle removal, as the initial boundary signal was saturated with spatial noise. Second, a dilation step was employed for restoring any boundary pixels that were removed during the erosion step, producing discontinuities on the contour signal. This pair of subsequent morphological operations (erosion-dilation) is called "closing" process and is typical of contour-related operations in image processing. The contour signal was further enhanced by employing a skeletonization filter for edge thinning.

The boundary itself was extracted by a separate contour-tracing algorithm that resulted in the creation of a set of subsequent "boundary" pixels, i.e., a complete 1-D representation of the shape of the drape object. This 1-D representation of the drape shape is in fact a parametric function in a 2-D space, which means that it can be transformed into Cartesian, polar or complex representation at any time. The extracted shape was corrected for geometric (lens) distortions using a custom barrel distortion correction model [R98]. Although this type of distortion is the most prevalent factor in CCD-based commercial cameras, the maximum spatial correction that was measured along radial axes was about 3 pixels or less, i.e., 740 μm at most for the rescaled version of the drape images[2], which is still considered too small for the major shape features of the drape object in this study.

The resulting shape signal was subsequently interpolated in complex form, using standard bicubic spline interpolation. This spline representation was essential in order to acquire the drape boundary in analytical form, which is necessary for many derivative-based shape features in subsequent phases. The spline representation was also used for resampling and registration of a fixed number of reference points for the complete shape signal (256 points) for all drape images, regardless of the length or any remaining noise artifacts of the raw boundary signal itself.

The final result of this second phase of processing was a fixed set of reference points from the drape boundary, referring to the corresponding physical model of the fabric drape itself (analytical spline model, instead of sequence of pixels).

Figure 2 presents the basic approach employed for the Pre-Processing phase of this study. The labels *model.B1* and *model.B2* refer to the applied optimal designs of the corresponding *model.A1* and *model.A2* specifications (already identified during phase-1, see Figure-1).

The next five figures, i.e., Figure 3 through Figure 7, illustrate the intermediate stages of image pre-processing according to the procedure described in Figure 2. In Figure 3, the original drape image is displayed as it is contained in the image database (SL set). Figure 4 shows the cropped ROI in 8-bit grayscale, as it is used in the following processing steps, while the red point shows the detected center of the drape object. Figure 5 presents the intermediate stage of drape object segmentation (from the background), i.e., after the completion of the blue boxes of model.B1 in Figure 2. In Figure 6, model.B1, model.B2 and spline interpolation steps have been completed; the green continuous line represents the final drape boundary that was detected and the red dotted line is the spline

[2] Rescaled images: 250 mm ↔ 1024 pixels ⇒ 4.096 pixels/mm, thus 3 pixels is: 0.732 mm or 732 μm.

interpolation function that describes this boundary in analytical form. Finally, in Figure 7 all the previous results are combined and overlaid on the 8-bit grayscale cropped ROI; the blue radial sections describe angular exclusion areas to avoid false detection of boundary points (supporting base) and the corresponding “dead-zones” spline function is presented in yellow dotted line, while the normal spline function is presented in green dotted line; the red squares on the boundary represent the detected low and high peaks, which define the location of the actual drape folds (high peaks).

Phase-2: Pre-Processing

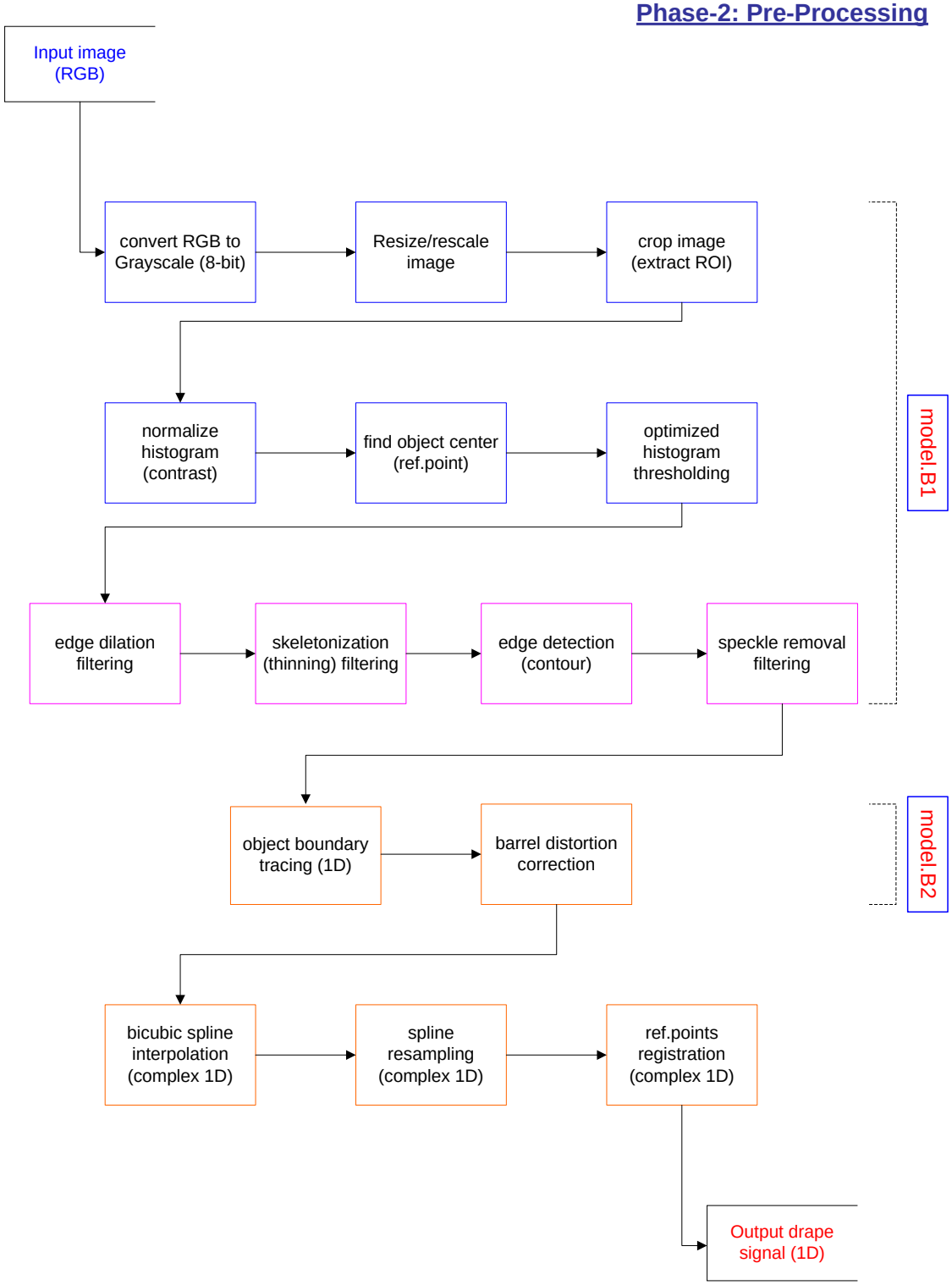

Figure 2: Basic approach employed for the Pre-Processing phase of this study.

Figure 3: Original drape image as it is contained in the image database (SL set).

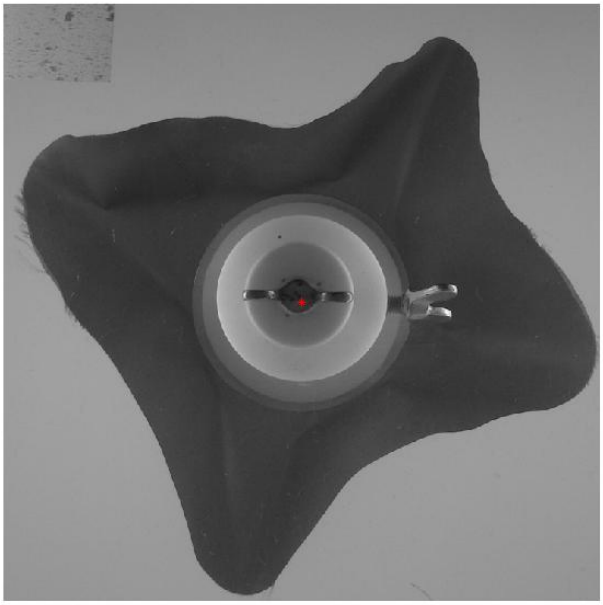

Figure 4: Cropped ROI in 8-bit grayscale used in the following processing steps.

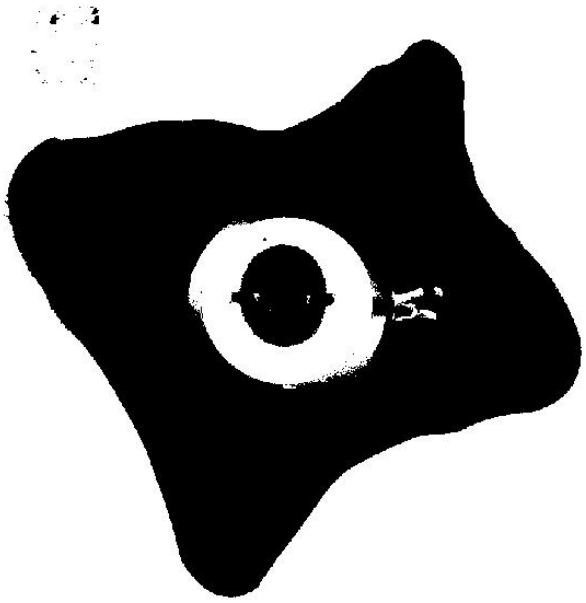

Figure 5: Intermediate stage of drape object segmentation (see: model.B1).

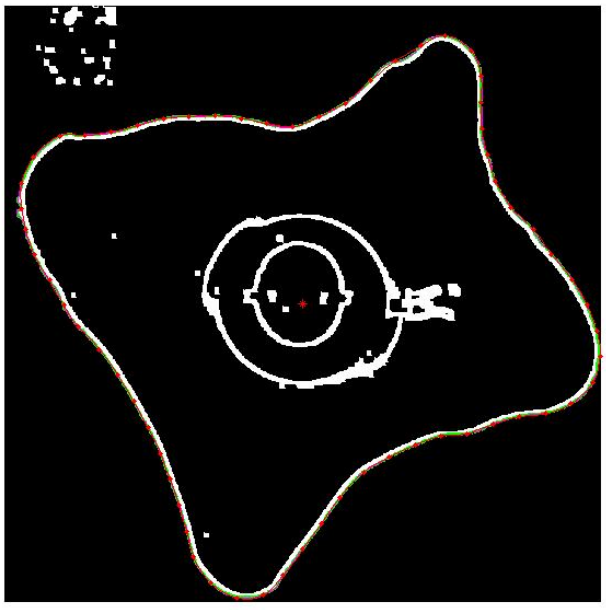

Figure 6: Geometric corrections, boundary detection (green line) and spline interpolation (red line) steps completed; boundary shape is ready for registration.

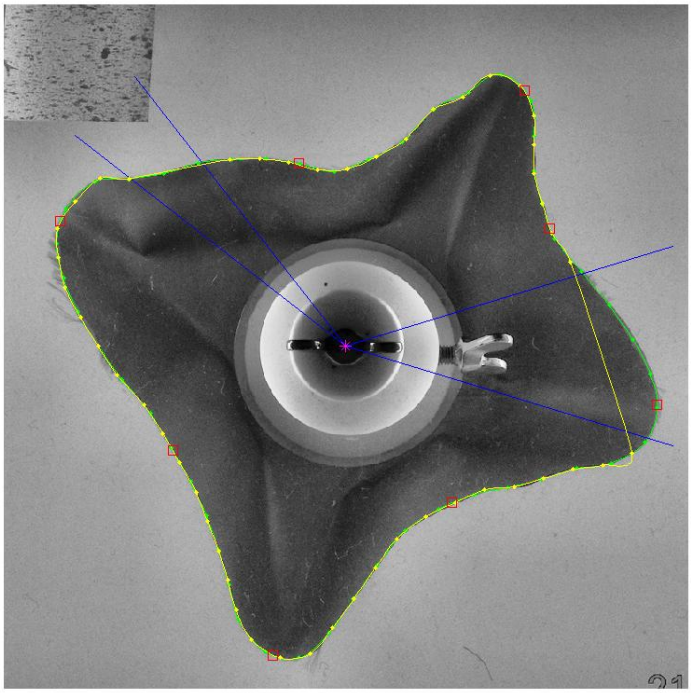

Figure 7: Combined and overlaid drape boundary detection results on the 8-bit grayscale cropped ROI. The blue radial sections describe angular exclusion areas for the "dead-zones" spline function presented in yellow dotted line, while the normal spline function is presented in green dotted line. The red squares on the boundary represent the detected low and high peaks, which define the location of the actual drape folds (high peaks).

Due to deficiencies in the acquisition process of the drape images, the SL set was not exploited to its full extend. Specifically, 140 out of 335 drape images in the SL set was excluded from all the subsequent phases of this study, due to improper coloring (fabric/background), non-correctable artifacts from the supporting mechanisms of the experimental setup or low-quality image segmentation. The final set of 195 drape images was considered adequate for the purposes of this study, in terms of size and unbiased statistical distribution of various types of drape objects.

2.3 Phase-3: Categorization-Prediction

The Categorization-Prediction phases of this work resulted in the design, implementation and testing of various classification and regression models, based on a wide set of shape features that were used as shape descriptors or "signatures" of the drape boundary.

First, the registered spline function of the drape boundary was used to calculate the same spatial signal in multiple representations, specifically in Cartesian, polar and complex forms. Although most shape features were defined upon the radial-angular representation of the boundary, these multiple representations were necessary to serve as the base data for some of the shape descriptors (e.g. spectral analysis). In all cases, the base signals were normalized before any further processing, to ensure invariance against possible rescaling of the drape database images.

The set of shape descriptor candidates included a total of 129 shape feature functions, selected from typical contour-based, region-based, spectral or higher-order curve functions [R00]. In most cases, each shape feature was encoded as an 8-value vector by employing eight standard statistical measures, presented in Table 2. The complete list of all the 129 shape features employed in this study is presented in Table 3.

The new dataset of composite shape features vectors were subsequently used as the base data for developing classification and regression models. These models were employed as the final stage of the overall drape image analysis system, using content-related characteristics of the drape object to predict its corresponding physical (fabric) properties or classify it into one of the available pre-defined categories of fabrics with known properties.

The two primary models selected for this task were: (a) Classification and Regression Trees (CART) and (b) weighted k-nearest neighbors (w/Knn) [R08]. These two models were used for both classification and regression predictors. Additional models were used for specific data analysis tasks, such as T-test, F-test and MANOVA [R12] for statistical significance analysis and feature rankings, as well as the k-means algorithm for data clustering [R08].

Table 2: Standard statistics used to encode each shape feature function as a single 8-value vector.

Standard statistical measures for features
mn : minimum value of input signal
mx : maximum value of input signal
rng : range of values of input signal
avg : mean value of input signal
sdv : stdev value of input signal
skw : skewness value of input signal
kur : kurtosis value of input signal
ent : entropy value of input signal

Using the results from previous studies [R99], the first experiments included direct classification tests against the three primary drape shape categories, i.e.: (i) “marked”, (ii) “less-marked”, (iii) “slight”. However, it soon became clear that the categorization of the drape samples into these three rough categories was not appropriate for the shape features dataset that was constructed during phase-2 of this study. Specifically, both statistical significance analysis and plots of individual shape features against these three categories showed that there was excessive overlapping and intra-class statistical error was too large. These experiments were extended by employing a more detailed 23-class categorization that was provided together with the FL database [R99]. This scheme was repeated with k-means clustering for re-distributing the drape samples into 15 to 25 new clusters. In all cases, the statistical error remained excessively high due to large intra-class overlapping. These preliminary results confirmed that classification and/or clustering of the drape samples using the constructed dataset of shape descriptors was inefficient, in terms of providing the means to “predict” the physical characteristics of an unknown fabric based on its drape image.

Table 3: Standard statistics used to encode each shape feature function as a single 8-value vector. Value at offset 01 is reserved for sample reference (imageID).

Composite shape features vector with all the calculated values	
02..09	: base stats for C data series
10..17	: base stats for X data series
18..25	: base stats for Y data series
26..33	: base stats for R data series
34..41	: base stats for half-spectrum of C data series
42..44	: exp.regr.func parameters of half-spectrum of C
45..52	: base stats for half-spectrum of R data series
53..55	: exp.regr.func parameters of half-spectrum of R
56..63	: base stats for Fourier descriptor series of (R,A)
64..66	: exp.regr.func parameters of half-spectrum of FD
67..74	: base stats for R-based curvature data series
75..82	: base stats for XY-based curvature data series
83	: number of zero-crossings against mean value in R
84..91	: base stats for 1st derivatives of R at zero-crossings
92..100	: base stats for weights (sin(AoA)) of R at zero-crossings
101	: number of signal peaks (inward/outward folds) in R
102..109	: base stats for R at signal peak points (only)
110..117	: base stats for angular distribution of signal peaks
118..125	: base stats for inertia moments of signal at peak-point axes

126	: min/max ratio of inertia moments of signal at peak-point axes
127	: total length (perimeter) of signal curve
128	: total area (enclosed) of signal curve
129	: area ratio parameter of signal curve
130	: circularity parameter of signal curve

Based on these preliminary results, it was decided that direct prediction of specific physical parameters of the fabric itself should be developed through appropriate regression models, since this approach would not require prior categorization of the drape images into fixed classes/clusters. The two selected models, CART and w/Knn, were applied as regressors for three important specific fabric parameters from the FL database: (a) "weight", (b) "avg. bending rigidity" and (c) "avg. shear rigidity".

For CART, the complete set of 129 features was used for training purposes, in order to analyze in parallel the informative content or "importance" of each shape feature. The dataset of 195 drape images (see section 2.2) was used with k-fold cross-validation techniques [R08] in order to ensure robust and statistically significant results. Experiments with CART regression models were repeated with various configurations and selection of model parameters. The regression error was considered in terms of Mean Absolute Prediction Error (MAPE) in the normalized output range, therefore the value of MAPE can also be considered as a rough estimate of the relative error (%) of the predicted values.

Similarly to the CART, the w/Knn model was used in the form of a regressor, i.e., employing local averaging on the k closest "neighbors" of the current input sample, with an option of weighting profile against the distances ("closeness"). Due to the nature and complexity of w/Knn, a feature pre-selection step was employed in order to limit the dimension of the input vector to the top-10 (best) features, using a typical T-test univariate procedure for feature ranking [R08]. As in the case of CART, the dataset of 195 drape images (see section 2.2) was used with k-fold cross-validation techniques [R08] in order to ensure robust and statistically significant results. Experiments with w/Knn regression models were repeated with various configurations and selection of model parameters, and the regression error was considered in terms of Mean Absolute Prediction Error (MAPE) in the normalized output range.

Figure 8 illustrates the overall process of phase-3, i.e., the shape feature extraction, statistical analysis and categorization-prediction through regression models.

Phase-3: Categorization-Prediction

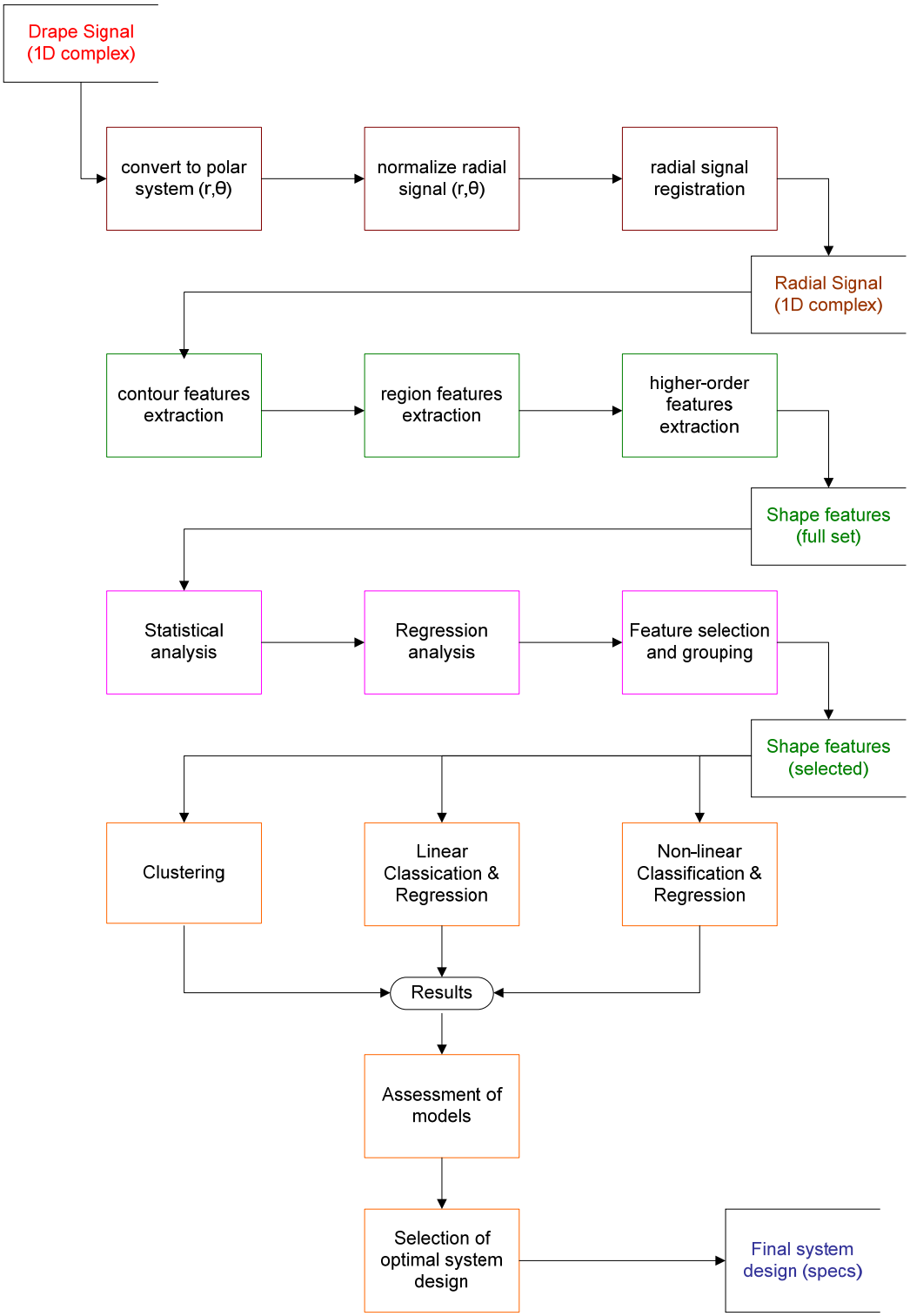

Figure 8: Basic approach employed for the Categorization-Prediction phase.

3. Results

The two selected models, CART and w/Knn, were applied as regressors for three important specific fabric parameters from the FL database: (a) "weight", (b) "avg. bending rigidity" and (c) "avg. shear rigidity".

3.1 CART regression models

Table 4 presents the final results of the CART regression experiments. The labels *Dataset=FL* and *Dataset=DZ* refer to using the normal (full) or "dead-zone" limited version of the spline boundary functions. The k-fold cross-validation was applied for k=195 (leave-one-out mode), k=65 and k=39. The average and stdev values of MAPE have been calculated for each k-fold mode and for all k-fold modes. Red numbers indicate best prediction performance for the specific fabric parameter using the CART regression model.

Table 4: Final results of the CART regression experiments. Red numbers indicate best performance for the specific fabric parameter using the CART regression model.

RESULTS: CART regressors

Target: drape col.#09 (Weight)
Setup: CART/deviance/splitmin=10/Dataset=DZ

MAPE:	Mean	Stdev
leave-one-out	0,19196	0,17600
kfolds=65	0,19195	0,10100
kfolds=39	0,19580	0,07700
AVG:	0,19324	0,11800

Target: drape col.#09 (Weight)
Setup: CART/deviance/splitmin=5/Dataset=DZ

MAPE:	Mean	Stdev
leave-one-out	0,19331	0,17500
kfolds=65	0,19215	0,10600
kfolds=39	0,19635	0,08400
AVG:	0,19394	0,12167

Target: drape col.#17 (Bending Rigidity)
Setup: CART/deviance/splitmin=10/Dataset=FL

MAPE:	Mean	Stdev
leave-one-out	0,12126	0,20801
kfolds=65	0,12042	0,12743
kfolds=39	0,11985	0,08744
AVG:	0,12051	0,14096

Target: drape col.#17 (Bending Rigidity)
Setup: CART/deviance/splitmin=5/Dataset=DZ

MAPE:	Mean	Stdev
leave-one-out	0,10287	0,19419
kfolds=65	0,10279	0,10635
kfolds=39	0,10682	0,08471
AVG:	0,10416	0,12842

Target: drape col.#22 (Shear Rigidity)
Setup: CART/gdi/splitmin=10/Dataset=FL

MAPE:	Mean	Stdev
leave-one-out	0,08214	0,12305
kfolds=65	0,08682	0,07955
kfolds=39	0,08172	0,06148
AVG:	0,08356	0,08803

Target: drape col.#22 (Shear Rigidity)
Setup: CART/gdi/splitmin=5/Dataset=FL

MAPE:	Mean	Stdev
leave-one-out	0,08901	0,13298
kfolds=65	0,09245	0,08054
kfolds=39	0,09131	0,06133
AVG:	0,09092	0,09161

Figures 9 through 11 illustrate the error distribution function of the optimized CART regressor for each of the predicted fabric parameters, based on the corresponding k-fold cross-validation errors.

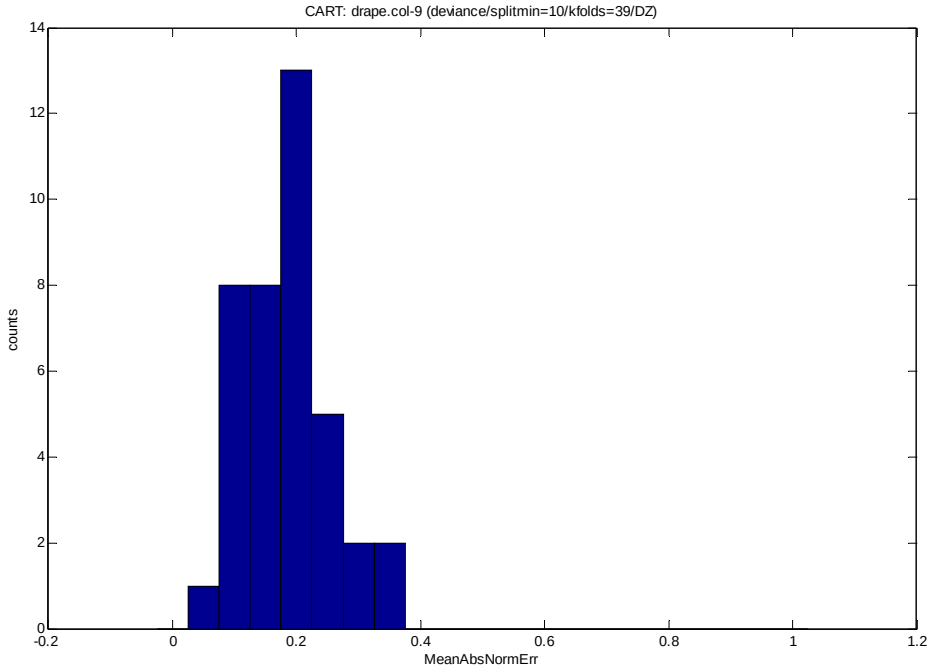

Figure 9: CART regressor errors for the “weight” parameter.

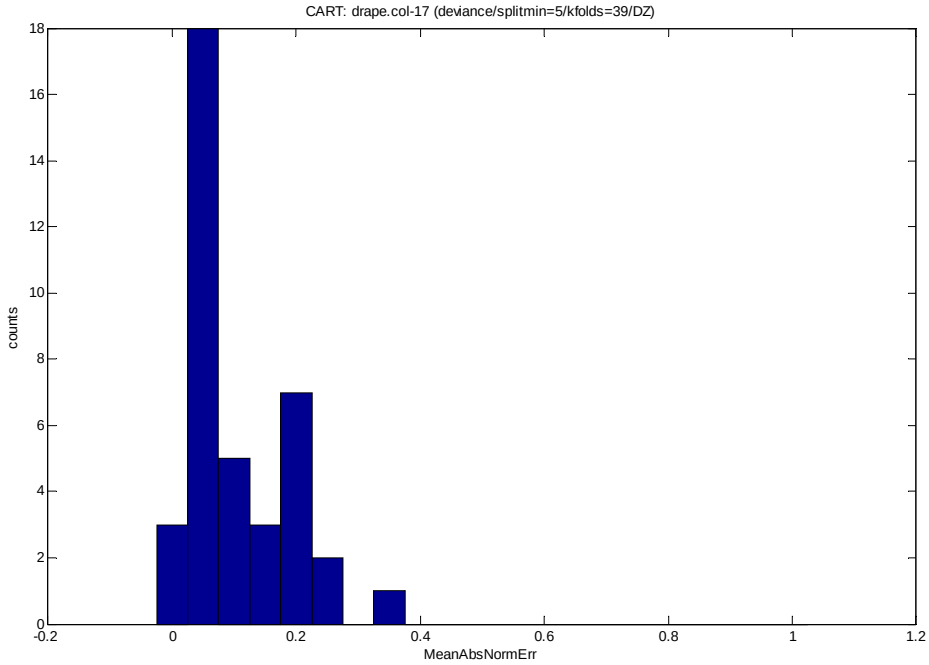

Figure 10: CART regressor errors for the "bending rigidity" parameter.

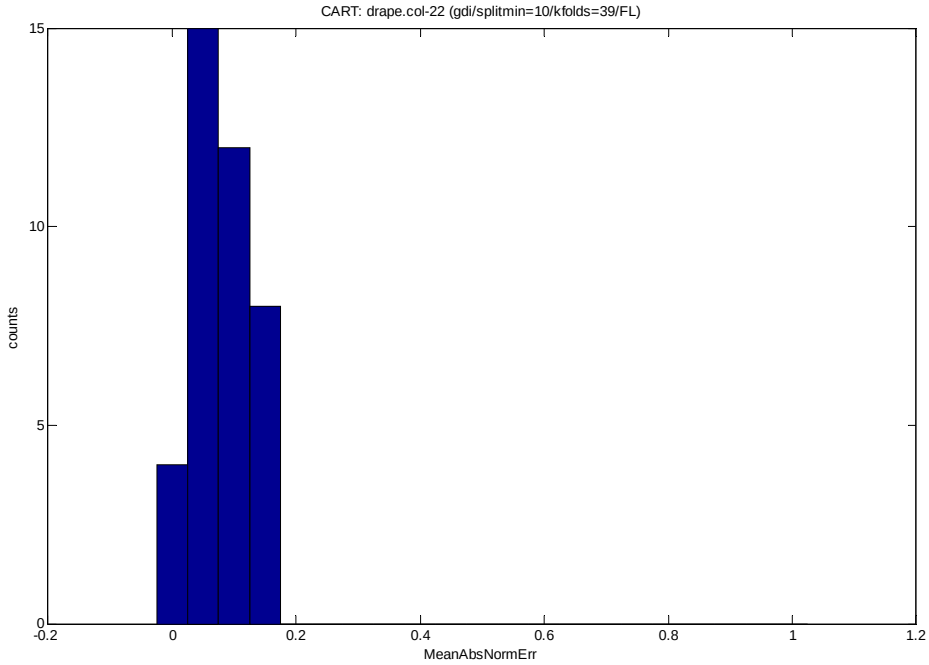

Figure 11: CART regressor errors for the "shear rigidity" parameter.

3.2 w/Knn regression models

Table 5 presents the final results of the w/Knn regression experiments. The labels *Dataset=FL* and *Dataset=DZ* refer to using the normal (full) or "dead-zone" limited version of the spline boundary functions. The k-fold cross-validation was applied for k=195 (leave-one-out mode), k=65 and k=39. The average and stdev values of MAPE have been calculated for each k-fold mode and for all k-fold modes. Red numbers indicate best prediction performance for the specific fabric parameter using the w/Knn regression model. Yellow background indicates performance better than the corresponding CART regressors.

Table 5: Final results of the w/Knn regression experiments. Red numbers indicate best performance for the specific fabric parameter using the CART regression model. Yellow background indicates performance better than the corresponding CART regressors.

RESULTS: w/Knn regressors

Target: drape col.#09 (Weight)
Setup: wKnn/chebychev/gauss/K=5/Dataset=FL/fset=Uvar.top-3

MAPE:	Mean	Stdev
leave-one-out	0,16241	0,13859
kfolds=65	0,16767	0,08663
kfolds=39	0,16837	0,06755
AVG:	**0,16615**	**0,09759**

Target: drape col.#17 (Bending Rigidity)
Setup: wKnn/cityblock/none/K=1/Dataset=FL/fset=Uvar.top-10

MAPE:	Mean	Stdev
leave-one-out	0,06485	0,11020
kfolds=65	0,06507	0,06600
kfolds=39	0,06598	0,05017
AVG:	**0,06530**	**0,07545**

Target: drape col.#22 (Shear Rigidity)
Setup: wKnn/cityblock/gauss/K=3/Dataset=FL/fset=Uvar.top-10

MAPE:	Mean	Stdev
leave-one-out	0,07496	0,10835
kfolds=65	0,07470	0,05950
kfolds=39	0,07576	0,04748
AVG:	**0,07514**	**0,07178**

Figures 12 through 14 illustrate the error distribution function of the optimized w/Knn regressor for each of the predicted fabric parameters, based on the corresponding k-fold cross-validation errors.

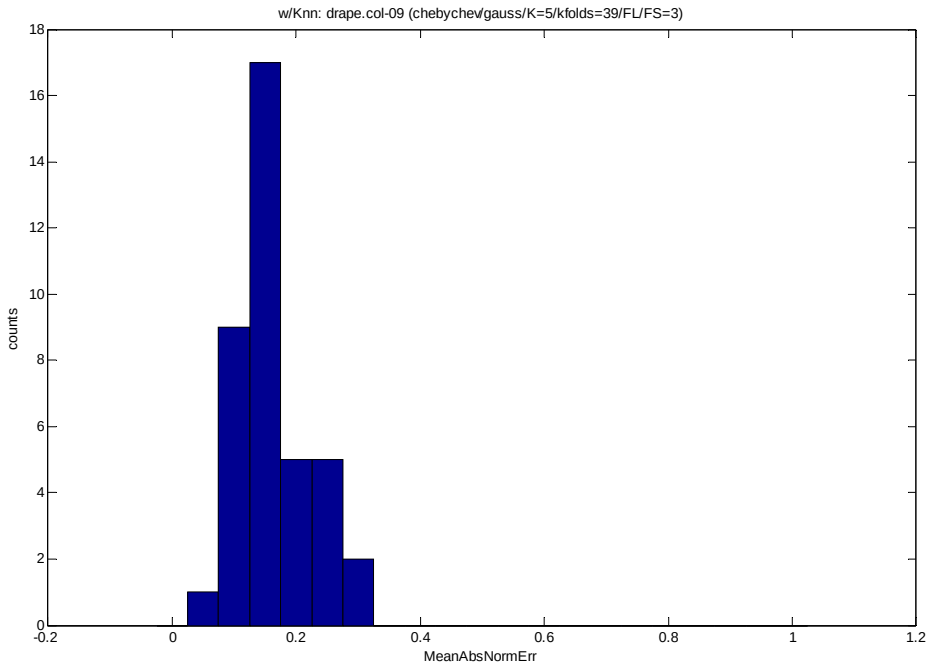

Figure 12: w/Knn regressor errors for the "weight" parameter.

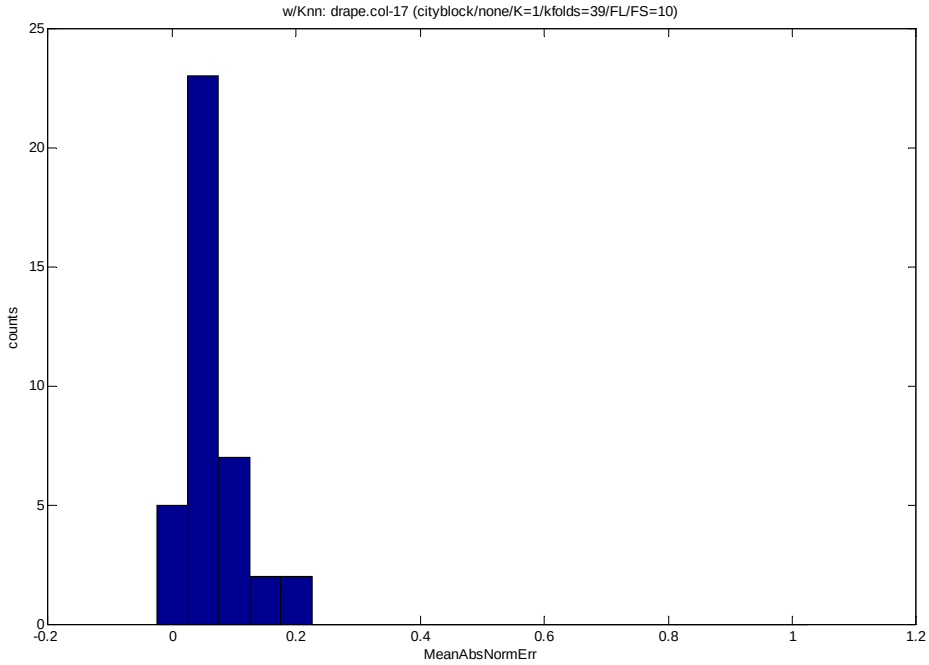

Figure 13: w/Knn regressor errors for the "bending rigidity" parameter.

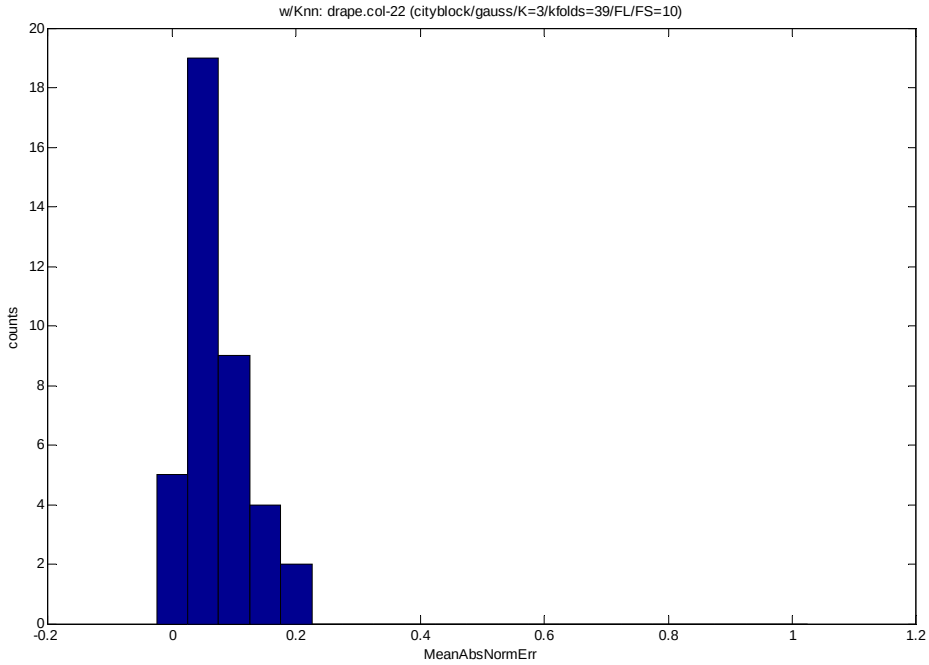

Figure 14: w/Knn regressor errors for the "shear rigidity" parameter.

4. Discussion

Results from both statistical analysis and from the regression models (CART, w/Knn) proved the feasibility of the proposed system, i.e., using automated image analysis for shape features extraction from the drape boundary, in order to predict specific physical parameters of the tested fabric itself.

4.1 Prediction error, shape features, stability

Although rigid categorization of fabrics into fixed classes has not proven effective, neither with pre-defined classes or clustering-based approaches, regression models have been proven successful in predicting "weight", "bending rigidity" and "shear rigidity" with acceptable error. In all three cases, the minimum prediction error (MAPE) was achieved by w/Knn regressors, closely matched by the corresponding CART regressors.

The maximum prediction error (MAPE=0.16615, see: Table 5) was calculated for the "weight" fabric parameter, however this specific parameter relatively easy to estimate in practice and it was used primarily as a reference factor for the performance of regression models, since it exhibits low statistical correlation with the drape shape compared to the other two "rigidity" parameters. This assertion was confirmed by the corresponding prediction errors of these two parameters, i.e., "bending rigidity" and "shear rigidity" (MAPE=0.06530 and MAPE=0.07514, see: Table 5).

Analysis of the error distributions (MAPE histograms, see: Figures 9-14) in k-fold cross-validation tests confirmed that the performance of both the CART and w/Knn regression models were stable and robust in terms of the validity of the predicted value for all three physical parameters. This means that the estimated prediction errors can be considered statistically significant, provided that the original dataset is "complete" and "unbiased", i.e., it contains more or less the same number of representatives from all the fabrics.

4.2 Imaging recommendations

The most difficult part in the development of this system was the design of the pre-processing stages of image analysis. This is due to the fact that the original drape images contained in the FL database exhibited many deficiencies in terms of correct capture of the drape object (fabric shadow and perimeter). The problems can be grouped into imaging-related, cloth-related and equipment-related. In short, the list of major issues is:

1. Cloth color confusion: Many sample images contained semi-transparent, non-uniform or same-color (with background) cloth samples, which made the whole segmentation process extremely difficult to automate.

2. Screw distortion: Many sample images contained drapes that are partially obstructed by the fixed mechanism (metallic screw), which created significant information loss inside and around these areas (no boundary).

3. Non-uniform illumination: Background was illuminated in a non-uniform way, especially near the corners and the border of the box.

4. Calibration box distortion: Some sample images with wide-angle drapes had their top-left section partially obstructed by the calibration box, which created information loss inside and around these areas (discontinuities).

5. Non-trimmed cloth samples: The presence of floating fibers around the drape shape created false boundary indications in some samples.

Some of these issues were addressed in various ways, e.g. using "dead-zone" angular sections to overcome issues #2 and #4, but with significant loss of boundary data (see: Figure 7, yellow dotted line). However, the most effective way to correct these problems is to modify the experimental protocol and the equipment used for creating the dataset of drape images.

A suggestive list of proposals for better imaging is:

- Blue/Green BG: Exploit full RGB potential and use pure "green" or "blue" background, in order to make image thresholding much simpler. This setup should make sure that no transparent clothes or clothes with color similar to the background are used. If necessary, more than one alternative background could be used, for different sets of cloths.

- Screw distortion: Make sure every sample is well-fit onto the fixed plate with no obstruction from the screw before taking the image. This means that the whole mechanism should be "included" inside the drape's shadow, so that it does not cause any discontinuities to the drape boundary. Painting the screw mechanism in a non-illuminating (non-metallic) color, e.g. pure black or same as the background, could also help the segmentation process, since it could be easily excluded from the drape object area.

- Flat-field correction: Image restoration (illumination, noise, etc) requires a complete set of "empty" images, i.e., with no cloth sample present (only fixed mechanism + background) and well-illuminated plane. This is a one-time procedure which is typical in many imaging applications, like in X-ray digital radiography or aerial photography, and it should be considered as part of the calibration camera process.

- Camera calibration: Instead of the calibration box (top-left), which may obstruct view, instead a set of reference points can be present all around the outer box (panel edges), for better model approximation. Moreover, a one-time procedure should be defined together with a full-field calibration template (e.g. a grid or a set of patterns), in order to provide adequate information for flat-field and geometric corrections.

- Fixed camera position: In the current database, image center differs slightly between samples, mostly because of some non-constant tilt of the

- camera. Using a camera fully embedded in the system should fix similar problems that cause non-stationarity problems (inherent statistical errors in the estimated correction models).
- Well-trimmed cloth samples: Some of the problems with noisy boundary shapes have been identified as the result of non-sharp cloth edges (see: Figure 7, top-left peak). It is suggested that all cloth samples are cut with very sharp edges (i.e., no loose fibers) or even wetted cloth edges (but not too much so that it alters the physical properties of the cloth, e.g. weight).

4.3 Example of drape image processing

A full example of drape image processing is presented here. The image file "E0035A_5.jpg" from the single-layered (SL) samples of reference fabrics in the Fabrics Library (FL) is used as input in the pre-processing module of the system. Figure 16 illustrates the real output of the main program (Matlab console). Figure 17 and Figure 18 present the final output of the system after pre-processing (segmentation) and shape features extraction stages.

```
>> demo1_drapeimg_proc
Drape Image Processing (DIP) - Boundary Extraction DEMO
Harris Georgiou (c) 2008, mailto:xgeorgio@di.uoa.gr
-------------------------------------------------------

initializing...

reading image file: 1 of 1 (F:\Library\DrapeDB\img\SLdemo\E0035A_5.JPG)...done
performing image resizing and cropping...done
performing image contrast enhancement...done
performing image thresholding...done
performing edge filtering...done
performing image closure filtering...done
performing boundary tracing...done
calculating barrel-corrected boundary...done
calculating spline approximation of boundary (full mode)...done
plotting object boundary approximation and center (full mode)...done
calculating spline approximation of boundary (cutoff mode)...done
plotting object boundary approximation and center (cutoff mode)...done
```

detecting drape folds...done

Figure 16: Pre-processing and segmentation results from the first stage of the image analysis procedure for image file “E0035A_5.jpg”.

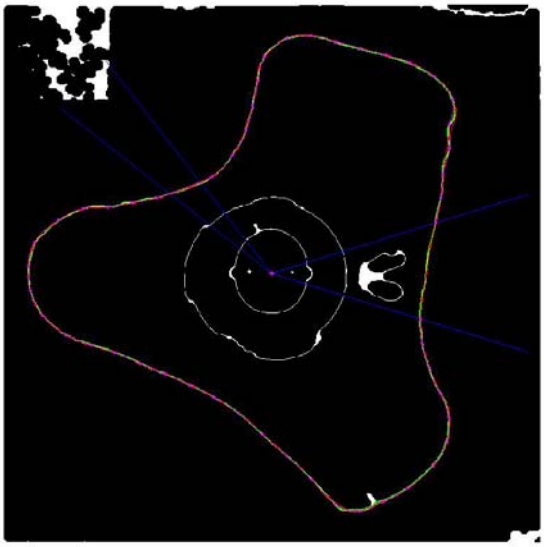

Figure 17: Pre-processing and segmentation results from the first stage of the image analysis procedure for image file “E0035A_5.jpg”.

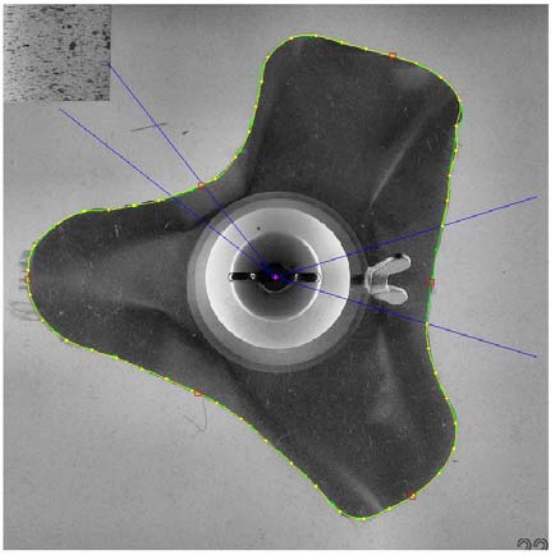

Figure 18: Results from the second stage of the image analysis procedure for image file "E0035A_5.jpg". Red squares represent detected signal peaks (inner/outer folds of drape sample).

Table 8 illustrates the values of the extracted shape features and the corresponding true and predicted values of the three main physical parameters investigated in this study (weight, bending rigidity, shear rigidity). The exact selection and number of the features used in each configuration are case-specific and they are also presented along with their exact values.

Table 8: Values of the extracted shape features and the corresponding true and predicted values of the three main physical parameters investigated in this study (weight, bending rigidity, shear rigidity) for drape image file "E0035A_5.jpg". All feature and parameter values are normalized in their min-max range.

Parameter	shape feature vector	regression results
Weight (true value = 57)	{f027, f039, f113} = (0,7169 0,5149 0,3299)	pred.value = 0,0957 true.value = 0,0000 abs.error = 0,0957 (9,57%)
Bending Rigidity (true value = 2,2)	{f126, f039, f113, f095, f045, f087, f114, f124, f028, f097} = (0,1278 0,5149 0,3299 0,2868	pred.value = 0,0018 true.value = 0,0467 abs.error = 0,0449 (4,49%)

	0,6408 0,2864 0,6636 0,4117 0,0771 0,1750)	
Shear Rigidity (true value = 157)	{f126, f113, f006, f039, f045, f095, f087, f114, f127, f124} = (0,1278 0,3299 0,5388 0,5149 0,6408 0,2868 0,2864 0,6636 0,4028 0,4117)	pred.value = 0,2994 true.value = 0,3416 abs.error = 0,0422 (4,22%)

5. References

[R00] Leapfrog – IP project: EC contract No. 515810 – NMP2-CT-2005-515810, Task 4.1 – "Material characterization for simulation and fabric selection", Sub-task 4.1.4: "Image Analysis Techniques for Material Characterization and Simulation", Project Scope Report and Preliminary Design, Revision: 1.0, 30-Apr-2007.

[R08] S. Theodoridis, K. Koutroumbas, Pattern Recognition, 3rd edition (Academic Press, San Diego, USA, 2006).

[R11] C.K. Park, S. Kim, W.R. Yu, Quantitative Fabric Drape Evaluation System Using Image Processing Technology (Part 1: Measurement System and Geometric Model), J. Testing and Eval., 32 (2) (2004)

[R12] W.W. Cooley, P.R. Lohnes, Multivariate data analysis (John Willey & Sons, New York, 1971).

[R13] R.C. Gonzalez, R.E. Woods, Digital Image Processing, 3rd edition (Prentice-Hall, New Jersey, 2006).

[R19] P. Pandurangan, J. Eischen, N. Kenkare, T. May-Plumlee, Mechanics of Fabric Drape – Part II: Generation of Optimal Simulations, College of Textiles, Univ. of North Carolina, 2004.

[R98] Janez Pers, Stanislav Kovacic, "Nonparametric, Model-Based Radial Lens Distortion Correction Using Tilted Camera Assumption", Technical Report, Univ. Ljubljana, Slovenia, 2002.

[R99] Leapfrog – IP project: EC contract No. 515810 – NMP2-CT-2005-515810, D4.2: Simplified Method to identify Material Characteristics, Hohenstein, May 2006.